Controlling the Composition Profile of Acrylic Acid Copolymers by Tuning the pH of Polymerization in Aqueous Dispersed Media

Clément Debrie, Noémie Coudert, Jabeen Abdul, Simon Harrisson, Olivier Colombani, Jutta Rieger

Controlling the composition profile of acrylic acid copolymers by tuning the pH of polymerization in aqueous dispersed media

Clément Debrie,[1] Noémie Coudert,[2] Jabeen Abdul,[1] Simon Harrisson,[3,*] Olivier Colombani,[2] Jutta Rieger[1,*]

[1] Sorbonne Université & CNRS (UMR 8232), Institut Parisien de Chimie Moléculaire (IPCM), Polymer Chemistry Team, 4 Place Jussieu, 75252 Paris Cedex 05, France

[2] Institut des Molécules et Matériaux du Mans (IMMM) UMR CNRS 6283, Le Mans Université, Avenue Olivier Messiaen, F-72085 LE MANS Cedex 9, France

[3] University of Bordeaux/CNRS/Bordeaux INP, UMR5629, Laboratoire de Chimie des Polymères Organiques, 16 Avenue Pey Berland, 33607 Pessac, France

sharrisson@enscbp.fr; jutta.rieger@sorbonne-universite.fr

Table of Contents (TOC) graphic

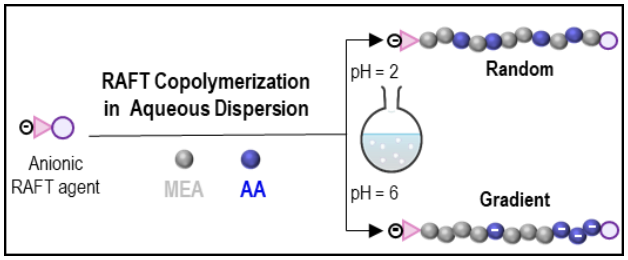

Abstract.

In radical copolymerization, the intrinsic reactivity of acrylic acid (AA) with a comonomer depends on its degree of ionization (α_{AA}). Furthermore, when monomers of different solubilities are copolymerized in a heterogeneous process, differences in partitioning between the continuous and discrete phase can result in apparent reactivity ratios that strongly differ from the intrinsic reactivity ratio observed in homogeneous solution. We demonstrate that this combination of chemical and physical contributions to the reactivity ratios of AA can be used to control the composition profile of acrylic acid copolymers in

RAFT-controlled aqueous heterogeneous polymerization. Specifically, RAFT-mediated copolymerizations of acrylic acid (AA) with comonomers of varying hydrophobicity were performed in water at different α_{AA} = 0 to 1 using a novel, water-soluble, sulfonate-functionalized trithiocarbonate chain transfer agent. A moderate decrease in reactivity of AA with increasing α_{AA} was observed in homogeneous conditions when AA was copolymerized with oligoethylene glycol acrylate (OEGA). A much greater change in apparent reactivity with increasing α_{AA} was observed with the more hydrophobic comonomers 2-methoxyethyl acrylate (MEA) and methyl acrylate (MA). This was attributed to partitioning of AA between the dispersed and continuous phases of these heterogeneous copolymerizations. Changing the pH of the reaction mixture thus allowed the synthesis of P(MEA-*co*-AA) and P(MA-*co*-AA) copolymers with very different composition profiles. In addition, when α_{AA} was changed *in situ*, block-like copolymers with similar overall AA content but different composition profiles were obtained. These differences in composition profile strongly impacted their thermoresponsiveness in water.

1. Introduction

The copolymerization of functional monomers allows the production of polymers with novel and tuneable properties[1,2]. These properties depend not only on the global copolymer composition, but also on the variation in composition between and within (e.g. random versus gradient) chains.[3] In free radical copolymerization, the comonomers are typically consumed at different rates due to their differing reactivity and selectivity.[4] As a result, the molar fraction (f_i) of the comonomers (M_i) in the feed varies over time. This in turn causes the composition of the polymer chains to vary as the polymerization proceeds (composition drift). In conventional radical polymerization, the lifetime of each chain is measured in milliseconds, and thus its composition represents a near-instantaneous snapshot of the monomer feed, while the polymerization may take several hours to reach completion. Changes in the molar ratio of comonomers throughout the course of the reaction will therefore result in the formation of a mixture of copolymers of different composition. In contrast, when reversible deactivation radical polymerization techniques (RDRP) are used, the total lifetime of each polymer chain (in both active and dormant states) is comparable to the duration of the reaction. Thus, variations in the monomer feed composition result in changes in the composition profile within each chain, forming spontaneous gradient copolymers. In batch processes, the composition profile is essentially determined by the reactivity ratios (r_1 and r_2) of the comonomer pair. Tuning the composition profile of a given copolymer (e.g. gradient towards random) typically requires complex monomer feeding processes,[5–7] which can be difficult to reproduce and depend on a large number of operational parameters.

Due to their pH-dependent ionization, carboxylic acid-functional comonomers such as acrylic acid (AA) or methacrylic acid (MAA) may (i) impart pH-responsiveness and negative charges to hydrophilic polymers, (ii) tune the transition temperature of LCST- or UCST-type polymers,[8] (iii) impact the aggregation extent[9] and morphology[3] of self-assembled amphiphilic block copolymers and (iv) render frozen block copolymer assemblies dynamic[10–12]. Such copolymers can readily be derivatized, for example by reaction with amines,[13] or decarboxylated to generate unsaturated, photocatalytically degradable polymer chains.[14,15] Moreover, AA can be obtained from lactic acid, a renewable feedstock.[16] The radical copolymerization of AA with numerous monomers, such as methyl methacrylate (MMA)[17],

n-butyl acrylate (nBA)[3], styrene[18–20], acrylamide[21,22] (Am), acrylonitrile[21] or *N*-vinyl pyrrolidone[23] (NVP) has been extensively studied in organic solution and in bulk[24], but there are far fewer reports of its copolymerization with hydrophilic comonomers in aqueous solution. In water the reactivity ratio of AA is pH-dependent, due to the pH-dependent deprotonation of AA (pKa ≈ 4.1)[25]. For instance, when AA was copolymerized with Am[26] or NVP[27] in water, increasing the pH from 2 to 5 led in both cases to a decrease in r_{AA} by a factor of 3-4. This can be attributed to the lower intrinsic reactivity of sodium acrylate (NaA) compared to AA due to inductive/mesomeric effect in the monomer and to the electrostatic repulsion between the growing chains and the negatively charged NaA monomer.[28–30]

AA is also commonly used in heterogeneous polymerization processes for the production of latexes (e.g. for adhesives, coatings etc.)[31]. Aqueous emulsion copolymerizations of AA with styrene[32–34], nBA[33], and vinyl acetate[35] have been extensively studied and the influence of various parameters, such as the type of emulsifier[36], the monomer concentration[34] and the pH[33], has been investigated. In these heterogeneous polymerizations, the main loci of polymerization are the particles that are formed during the earliest stages of the reaction. The observed reactivity ratios are *apparent* because, in addition to the changes in intrinsic reactivity described above, the comonomers partition to different extents between the different phases, leading to local concentration ratios that are very different from the global average. Strong composition drifts may thus occur during polymerization because of this partitioning effect, which generally outweighs differences in intrinsic reactivity[36,37] Moreover, changes in pH greatly affect the partitioning of AA/NaA between the different phases because the ionic NaA is less prone to enter the hydrophobic, monomer swollen particles than the neutral AA.[33] The copolymerization of AA with hydrophobic monomers (e.g. methyl methacrylate[38] or nBA[39]) has also been studied in alcohol/water mixtures, in which the monomers are soluble but the formed copolymers are not. When dispersion polymerization was combined with RDRP using reversible addition chain transfer polymerization (RAFT), the incorporation of AA in the copolymer and thus the composition profile of the polymers strongly depended on the EtOH/water composition of the polymerization medium.[39]

As polymer properties strongly depend on the chain's composition profile[3], it would be useful to develop scalable synthesis pathways allowing controlled insertion of carboxylic acid-functional monomers,

while maintaining control over molar mass and dispersity. We envisioned that such control might be possible using RDRP in aqueous dispersed medium, where monomer partitioning is a key determinant of the apparent monomer reactivity, simply by varying the pH and thus the degree of ionization of acrylic acid (α_{AA}). This novel approach would allow straightforward control over the composition profile of AA-containing copolymers with limited solubility in water.

In this work, we selected the RAFT-mediated copolymerization of AA and 2-methoxyethyl acrylate (MEA) in aqueous dispersion to demonstrate our concept. MEA is water-soluble and generates a hydrophobic, thermo-sensitive[40] and biocompatible[41–43] polymer. It has previously been used to generate amphiphilic block copolymer particles sterically stabilized by a hydrophilic block via polymerization-induced self-assembly (PISA).[44–47] To avoid the need for post-polymerization removal of the hydrophilic block necessary to obtain the desired statistical copolymer[48], we proposed to produce electrostatically-stabilized particles using a low-molecular weight, charged RAFT agent[49,50]. Thus, inspired by previous works on water-soluble RAFT agents[51–54], we designed a novel hydrosoluble RAFT agent functionalized by a sulfonate group that is negatively charged over a wide pH range (S-TTC, **Scheme 1** and **Scheme S1**). We then investigated the influence of α_{AA} on the copolymerization kinetics and copolymer composition profile. To simplify the following discussion, we will refer to changes in reactivity resulting purely from ionization, including changes in the distribution of electron density and repulsion between similarly charged chains and monomers, as changes in *intrinsic* reactivity. Changes in the extent of incorporation of AA that result from a combination of intrinsic reactivity and partitioning of the comonomers between the continuous and dispersed phases will be referred to as changes in *apparent* reactivity. The copolymerization of AA with MEA was compared to its copolymerization with two other acrylates that were more or less hydrophobic than MEA (methyl acrylate, MA, and oligoethylene glycol acrylate, OEGA, respectively) in order to distinguish the contribution of differences in *intrinsic* reactivity from those of *apparent* reactivity. Finally, we investigated the effect of varying α_{AA} during polymerization in order to impact *apparent* reactivity *in situ*. This allowed us to prepare copolymers of similar overall composition but with distinct composition profiles, resulting in different thermal and pH responses.

Results and discussion.

1.1. RAFT-mediated copolymerization of MEA and AA in aqueous medium at various α_{AA}

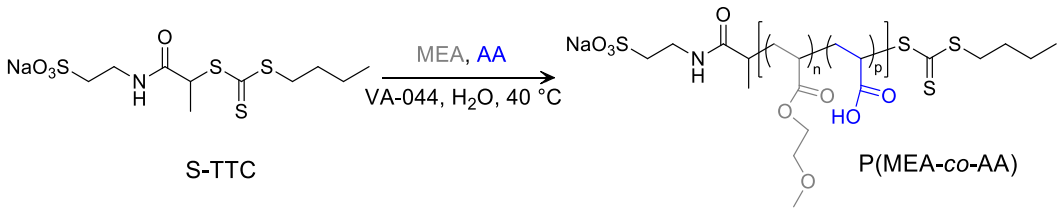

Scheme 1. Synthesis of P(MEA-*co*-AA) copolymers by RAFT-mediated polymerization using S-TTC.

Copolymerizations of MEA and AA were conducted in water at 40 °C using a novel sulfonated RAFT agent (S-TTC) and VA-044 as a radical initiator (**Scheme 1**). The RAFT agent was designed to be negatively charged and soluble over a wide range of pH, thanks to the strongly acidic character (pK_a ~ -1.6)[55] of the sulfonic acid, thereby improving the colloidal stability of aggregates of insoluble polymer chains[49]. In the first series of copolymerizations, α_{AA} was varied from 0 to 1 (**Table S1**). All other parameters were kept constant: the initial monomer feed composition ($f_{AA,0}$ = 0.1), the overall monomer concentration ($[monomers]_0 = [AA]_0 + [MEA]_0$ = 1.5 mol/L), and the targeted DP_n ($[monomers]_0/[S\text{-}TTC]_0$ = 100). The polymerizations started in heterogeneous conditions because they were conducted at 17 wt% in MEA, well above the maximum solubility of MEA (estimated to be 11 wt%[44] at 40 °C). In most polymerizations, the turbidity of the reaction media rapidly increased because of the formation of insoluble polymer that aggregated into particles large enough to strongly scatter light. Two polymerizations, A-0 and A-0bis, synthesized at $\alpha_{AA} \approx 0$, became clearer in the first hour of reaction, but subsequently became turbid.

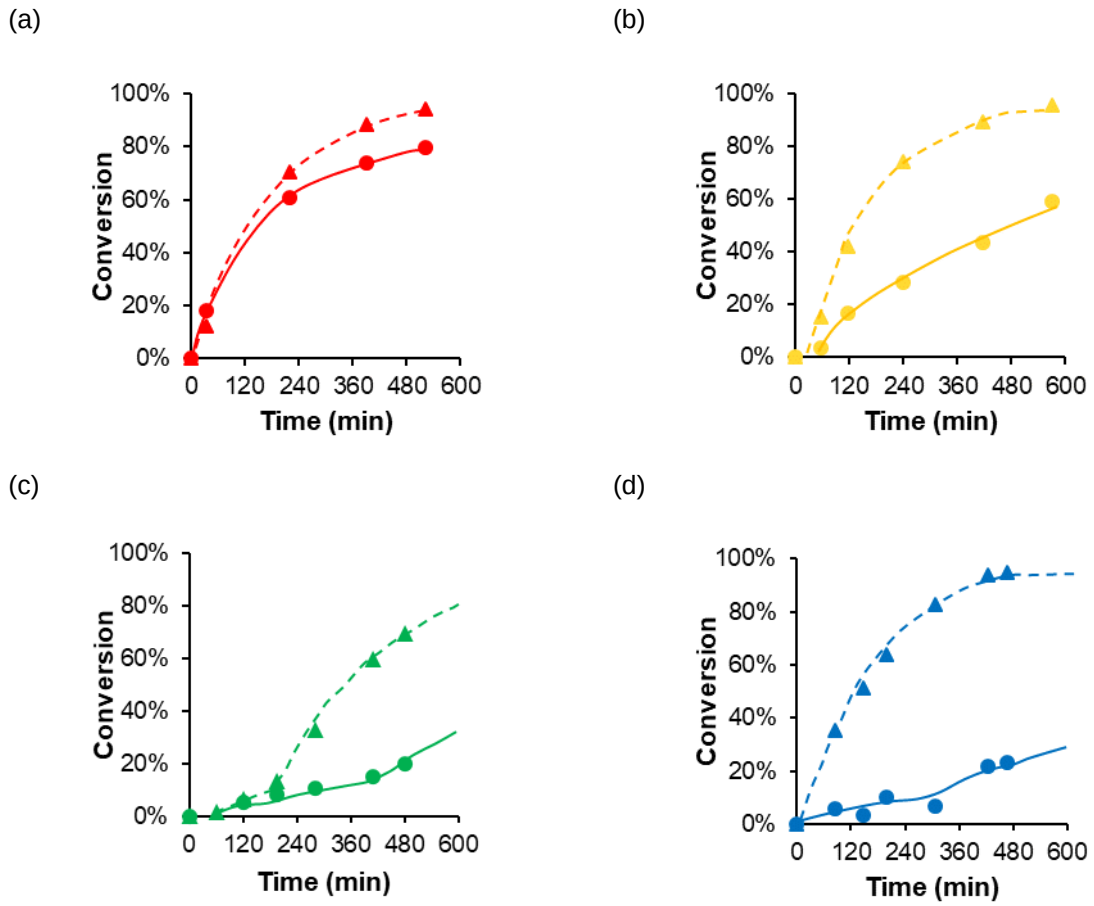

Figure 1. Kinetic monitoring of the first 600 min for copolymerizations conducted at different α_{AA}. Individual conversions in MEA (▲) and AA (●) are shown for (a) A-0 (α_{AA} = 0), (b) A-03 (α_{AA} = 0.34), (c) A-06 (α_{AA} = 0.60), and (d) A-1 (α_{AA} = 1). The dashed and solid lines are guides to the eye for the evolution of the conversion of MEA and AA, respectively. The complete kinetics of A-06 and A-1, and the -ln(1 – x) = f(t) plots of all samples are available in **Figure S3** and **Figure S4** respectively.

Throughout the polymerizations, aliquots were withdrawn and analyzed by ^{1}H NMR and size exclusion chromatography (SEC) to determine the overall and individual monomer conversions, and the number-average molar mass, M_n, and dispersity ($Đ$), respectively. Semilogarithmic plots (-ln(1 - x) = f(t)) are available in SI (**Figure S4**). While changes in polymerization rate are frequently observed in PISA dispersion polymerizations due to changes in the local monomer concentration resulting from particle formation[56], no significant change in slope was identified in the semilogarithmic plots of MEA conversion, except for sample A-06, where the presence of charged AA units in the chains certainly

delayed particle nucleation. For all other samples, the nucleation step presumably occurred for very short polymer chains and was therefore undetectable in the semilogarithmic plots.

As shown in **Figure 1**, the kinetics of AA strongly depended on α_{AA}, while the rate of conversion of MEA remained fairly constant. At $\alpha_{AA} = 0$, MEA and AA were consumed at similar rates, forming polymer chains that were initially water-soluble, and thus delaying the onset of particle formation. The monomers poly(ethylene glycol) acrylate and methacrylic acid are known to form hydrophobic domains through intermolecular interactions, leading to faster copolymerization: similar interactions may occur between MEA and neutral AA.[57] At $\alpha_{AA} = 0.34$, AA is consumed much more slowly than MEA. At $\alpha_{AA} = 0.60$, AA and MEA reacted at similar rates for the first 180 min (< 12% of global conversion), after which the rate of conversion of MEA accelerated while that of AA remained slow. At $\alpha_{AA} = 1$, significant conversion in AA (in its ionized NaA form) was only measured once x_{MEA} reached 95 %. Even at the start of the polymerization, when polymer chains were still water-soluble, the consumption of NaA was much lower compared to that of MEA.

A convenient way to quantify the variation of the reactivity of a monomer in a copolymerization is the Jaacks method[58] (see the Supporting Info, section 3, for more details), which can be used when the molar fraction of one monomer (AA, $f_{AA,0} = 0.1$) is small compared to that of the other (MEA). Importantly, as α_{AA} increases, the rate of AA consumption decreases, and the monomer feed becomes enriched in AA as the polymerization proceeds. As a consequence, points at high global conversion should be used with caution, as they may not satisfy the assumptions of the Jaacks method. However, as shown in **Figure 2**, good fits of the experimental data were obtained even at high global conversion, which may indicate a near-ideal polymerization ($r_{AA} \approx 1/r_{MEA}$): in this case, the Jaacks method is valid at all conversions, even when $f_{AA} >> 0.1$. The apparent reactivity ratio of MEA (r_{MEA}) increases significantly with the degree of ionization of AA: from 1.5 ± 0.2 at $\alpha_{AA} = 0$, r_{MEA} reaches 12.5 ± 1.3 at $\alpha_{AA} = 1$. These observations indicate that MEA preferentially homopolymerizes at high α_{AA}. Even though we cannot determine r_{AA}, we can reasonably assume that the reactivity of MEA is unchanged by α_{AA}, so that the increase of $r_{MEA} = k_{MEA\text{-}MEA} / k_{MEA\text{-}AA}$ actually results from a decrease of the reactivity of the AA monomers towards the MEA-terminated growing chains. These remarks and the much lower conversion rate of AA compared

to MEA with increasing conversion (**Figure 1**) both suggest that the apparent reactivity of AA decreases with increasing α_{AA}.

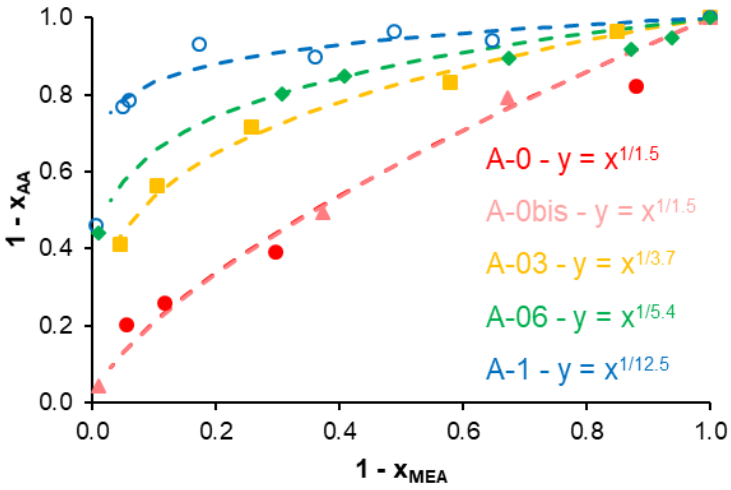

	α_{AA}	r_{MEA}	σ(r)
A-0	0	1.5	0.2
A-0bis	0	1.5	0.1
A-03	0.34	3.7	0.2
A-06	0.60	5.4	0.4
A-1	1	12.5	1.3

Figure 2. Jaacks plot for the copolymerizations conducted at different α: (a) A-0 (●, α_{AA} = 0), (b) A-0bis (▲, α_{AA} = 0), (c) A-03 (■, α_{AA} = 0.34), (d) A-06 (♦, α_{AA} = 0.60) and (e) A-1 (○, α_{AA} = 1). Curve fits (equations in the insert) are shown in dashed lines.

It has been reported that the propagation rate of sodium acrylate (NaA) homopolymerization ($k_{p,NaA}$) is one order of magnitude lower[59] than that of protonated AA ($k_{p,AA}$) as a result of the lower intrinsic reactivity of the acrylate ion towards radicals. Electrostatic repulsion between negatively charged propagating radicals and the deprotonated monomer also decreases intrinsic reactivity. Thus, as α_{AA} increases, there is a continuous decrease in intrinsic monomer reactivity. However, the effect observed in this work (variation of a factor 10) is much stronger than has previously been reported in homogeneous polymerizations (variation of a factor 3-4).[26–29,59] We hypothesize that an additional effect of monomer partitioning must be considered. In our system, the growing copolymers, while initially short and water-soluble, eventually become sufficiently hydrophobic to aggregate, leading to particle formation. At this point, the main locus of polymerization moves from the aqueous continuous phase to the hydrophobic discrete phase, and unreacted monomers partition between the two phases. In the discrete phase, the relative concentration of the charged NaA monomers should be reduced compared to MEA because it is entropically very demanding to confine the acrylate ions and their sodium counter-

ions in the hydrophobic polymer phase. The resulting reduction in local NaA concentration will further reduce the apparent reactivity of AA.

We therefore explain the strong impact of α_{AA} on the apparent reactivity of MEA during the RAFT dispersion polymerization of MEA and AA by a combination of monomer partitioning and changes in intrinsic reactivity, the former effect dominating. Because of the strong variation of apparent reactivity, the composition profile of the resulting copolymers should differ as a function of α_{AA} provided that the polymerization follows a controlled polymerization mechanism. As shown in **Figure S5**, the SEC traces of the formed copolymers were generally narrow and the experimental molar masses were in agreement with the theoretical values (**Table S1**). In addition, the main chain distribution absorbed at 309 nm (**Figure S5b**), the maximal absorption wavelength of the trithiocarbonate (TTC) function, indicating the presence of a TTC chain end, and M_n evolved linearly with conversion (**Figure S7**), as expected in a RAFT-controlled polymerization. A small shoulder at high molar mass was, however, generally observed in the RI signal, but not in the UV signal, indicating the absence of TTC functional group on these higher molar mass chains. These chains had approximately twice the molar mass of the main population, suggesting that they were formed through chain termination by recombination.[44,45] Deconvolution of the SEC chromatograms further confirmed this assumption because the experimentally determined number of dead chains was of the same order of magnitude as the number estimated from the rate of radical generation (see Supporting Information, **Figure S6** and **Table S2** and discussion).

In order to exclude the possibility that this high molar mass shoulder results from uncontrolled or partially controlled homopolymerization of AA in the aqueous phase – which would imply that less, or even no, AA was incorporated within the main chain distribution – we analyzed the purified polymers by ^{13}C-NMR in methanol-d_4, and compared them to a PAA homopolymer (see **Figure S9**). This revealed a clear difference in chemical shift between the signal corresponding to the AA carbonyl of homopolymeric PAA (AA-AA-AA triad at 178.5 ppm) and the signal corresponding to the AA carbonyl (at 177.9 ppm) in samples A-0bis and A-1, suggesting the formation of statistical copolymers with

negligible amounts of homopolymeric PAA. We can therefore conclude that well-controlled copolymers of MEA and AA were obtained using the sulfonate RAFT agent S-TTC over the complete range of α_{AA}.

As a controlled RAFT-mediated polymerization mechanism was observed, the composition profile of the copolymer chains should vary as function of α_{AA}. To illustrate this, we simulated the composition profile of 100 chains using the experimentally determined apparent reactivity ratio of MEA for each α_{AA} tested and an arbitrary constant r_{AA} = 1 (**Figure 3**). The latter will have little influence on the composition profile as the AA content is low. At α_{AA} = 0, the distribution of AA units in the polymer chains is close to random, whereas at higher α_{AA}, the incorporation of the AA in the copolymerization is delayed leading to gradient- or block-like polymer chains. The higher α_{AA}, the stronger the gradient.

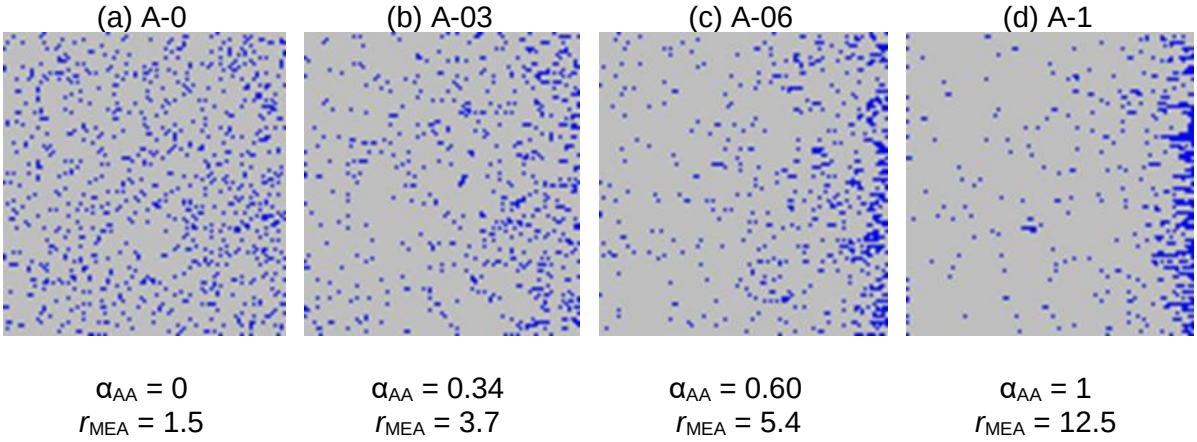

Figure 3. Simulation of 100 monodisperse P(MEA-*co*-AA) chains, stacked horizontally, each line on a figure corresponding to a different chain. The direction of polymerization is from left to right, MEA units are in grey and AA units in blue. Experimental $f_{AA,0}$, $DP_{n\,0}$, reactivity ratios of MEA and the final global conversion were used in the terminal model to determine the composition profiles (see SI).[24]

In order to distinguish the effects of the difference in intrinsic reactivity between AA and NaA from the effects of partitioning of the comonomers on their apparent reactivity, we performed copolymerizations of AA in homogeneous and heterogeneous conditions using different acrylate comonomers of similar chemical reactivity compared to MEA.

1.2. Influence of the heterogeneity of the polymerization process on kinetics

We first copolymerized AA with an oligoethylene glycol acrylate with 9 ethylene glycol moieties (OEGA) and then with methyl acrylate (MA). Both comonomers are acrylates with a structure similar to MEA, so their intrinsic reactivities should be similar. However, MA and OEGA are, respectively, more or less hydrophobic than MEA, as illustrated by their aqueous solubilities of around 6 wt% (MA) and > 70 wt% (OEGA) at 40 °C. POEGA is a water-soluble polymer, while PMA is not. Therefore, copolymerizations of AA with OEGA in aqueous solution are homogeneous, while copolymerizations of AA with MA are typically heterogeneous. Any changes in the apparent reactivity of AA relative to its copolymerization with MEA will thus be due to the presence or absence of a discrete polymer phase, and thus resulting differences in the local monomer concentrations. The molar feed fraction of AA and the targeted DP_n were kept constant at 0.1 and 100, respectively.

Three polymerizations were conducted with OEGA at α_{AA} = 0, 0.4 and 1 (samples B in **Table S3**). Near quantitative global conversions (x_{global} > 96 %) were achieved, while a broad shoulder was observed by SEC at higher molar mass, presumably due either to traces of difunctional monomer or to transfer reactions (see **Figure S10a**, **Table S3**). The conversion in OEGA evolved in a similar way at all α_{AA} (**Figure 4**). In contrast, AA was incorporated more slowly at α_{AA} = 1 than at α_{AA} = 0 or 0.4. The reactivity ratio of OEGA (r_{OEGA}) increased slightly with α_{AA}, from 1.3 (α_{AA} = 0) to 1.4 (α_{AA} = 0.4) and 2.4 (α_{AA} = 1) (**Figure S11**). As the copolymerizations were homogeneous, this increase in r_{OEGA} with α_{AA} cannot be ascribed to monomer partitioning. Thus, the intrinsic reactivity of OEGA and AA in water does indeed vary with α_{AA}, in agreement with previous works.[26–29,59] However, the variation is much weaker than the variation of apparent reactivity for the copolymerization of AA with MEA (r_{MEA} = 1.5 at α_{AA} = 0, 3.7 at α_{AA} = 0.34, and 12.5 at α_{AA} = 1). Additionally, the agreement between r_{MEA} and r_{OEGA} at α_{AA} = 0 is consistent with our assumption that the acrylates have similar intrinsic reactivities towards AA.

Copolymerizations with hydrophobic MA were carried out at α_{AA} = 0 and 0.4 (samples C in **Table S3**). High final global conversions (x_{global} > 84 %) were achieved and the SEC traces of the final samples were narrow and symmetrical indicating a good control over the polymerization (**Figure S10c**). The copolymerizations started in heterogeneous conditions (emulsion polymerization conditions, as monomer droplets were present). For both $\alpha_{AA,}$ the turbidity of the polymerization medium sharply

increased from slightly turbid to opaque (grey areas in **Figure 4**), indicating particle formation. The onset of aggregation at α_{AA} = 0 was more rapid than what had been observed in analogous copolymerizations with MEA, consistent with the greater hydrophobicity of MA. In these conditions, the copolymerization of MA and AA was essentially random, presumably due to the similar chemical structure of MA and AA, and because AA is protonated, i.e. neutral, and therefore able to diffuse quite easily into the particle cores. Thus, when AA is protonated, there is seemingly only a limited influence of the polymerization process (homogeneous for OEGA *vs.* heterogeneous for MEA and MA) on the apparent reactivity of the monomers. At intermediate α_{AA} (α_{AA} = 0.34), the conversion of AA was significantly retarded, reaching only 30 % over 32 h, while that of MA was essentially unaffected. Particle formation was delayed to monomer conversions > 31 % (**Figure 4b**), presumably due to the presence of charged monomer units in the polymer chains which compensates the lower content of AA units (F_{AA}) incorporated in the chains.

Overall, comparison of the different copolymerizations shows that the incorporation of AA in the growing chains is almost independent of the hydrophobicity of the comonomer at α_{AA} = 0, presumably because the molar ratio of neutral AA to hydrophobic comonomer within the copolymer aggregates is close to that of the feed. In contrast, at α_{AA} close to 0.4 the apparent reactivity of AA decreases with increasing hydrophobicity of the comonomer ($r_{OEGA} << r_{MEA} < r_{MA}$), probably because charged NaA is excluded from the main locus of polymerization. The resulting difference in relative monomer concentrations would amplify the differences in intrinsic reactivity caused by deprotonation, leading to strong variations of apparent reactivity.

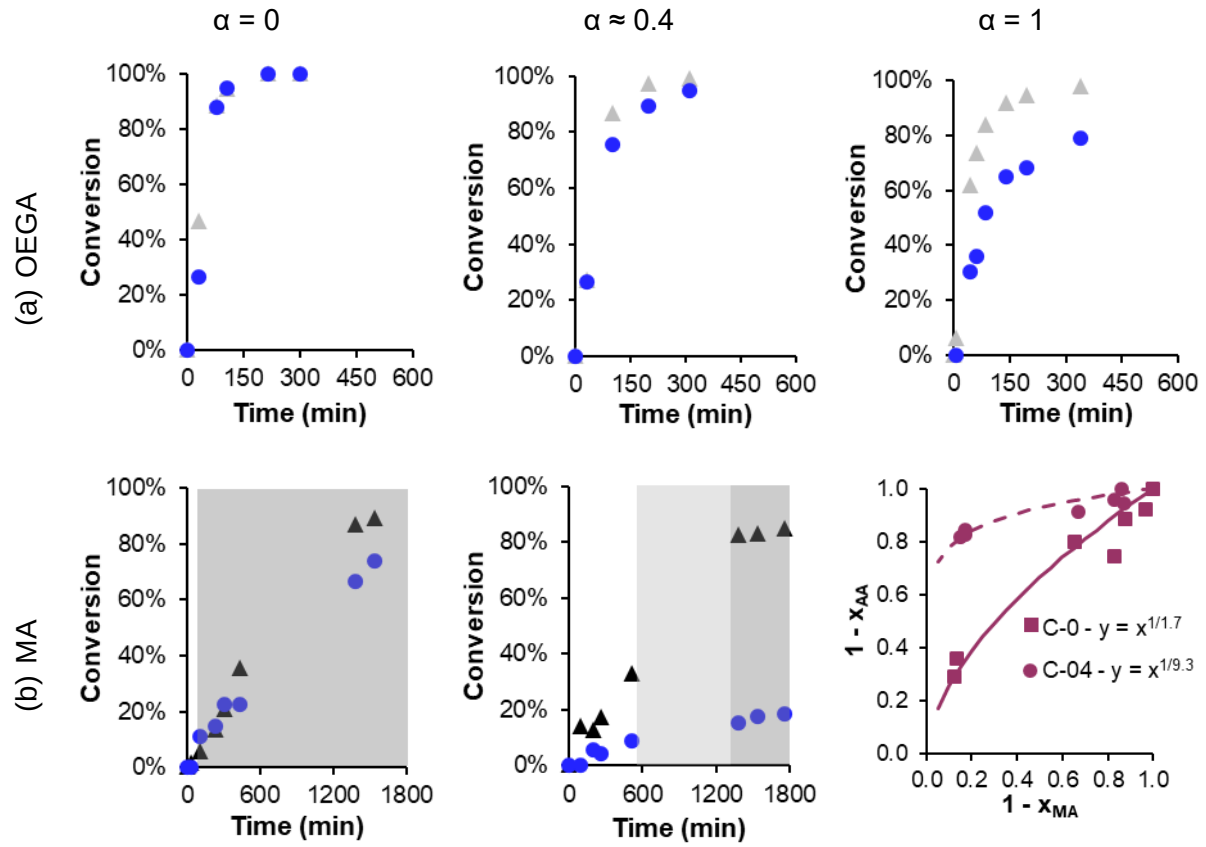

Figure 4. Kinetic monitoring of the copolymerizations of AA with (a) OEGA or (b) MA, in water at α_{AA} = 0, α_{AA} ≈ 0.4 and α_{AA} = 1 keeping constant $f_{AA,0}$ = 0.1 and $[monomers]_0/[S\text{-}TTC]_0$ = 100 (see **Table S2**). Individual conversions of OEGA or MA (▲) and AA (●) are shown. The dark grey areas indicate that a phase separation was observed. The onset of this phase separation occurred within the light grey areas, between two experimental points. Right: Jaacks plot for the copolymerizations of AA with MA conducted at α = 0 (C-0) and α_{AA} ≈ 0.4 (C-04).

Finally, to confirm that the chemical contribution (intrinsic reactivity) to the loss of reactivity of AA is negligible compared to the effect of monomer partitioning, we performed an additional copolymerization of MEA and AA in solution in DMF at similar intermediate α_{AA} of 0.34 (sample A-DMF in **Table S3)**. In these homogeneous conditions, the incorporation of AA was much faster than in aqueous dispersion. While r_{MEA} ~ 4 (**Figure 2**) in aqueous copolymerization of MEA/AA (α_{AA} = 0.34), it was only 1.8 (**Figure S11**) in DMF solution at identical α_{AA}, similar to the r_{OEGA} of 1.4 obtained for copolymerization of OEGA/AA in aqueous solution (α_{AA} = 0.44) (**Figure S11**).

1.3. Syntheses of block-like P(MEA-co-AA) copolymers through variation of α_{AA} during polymerization

We have shown above that changing α_{AA} strongly alters the incorporation of AA in the polymer chains, thereby resulting in copolymers with different composition profiles when the copolymers are prepared using a controlled polymerization technique. Notably, random or gradient-type copolymers, with a similar overall F_{AA}, can be synthesized at α_{AA} = 0 or 0.60, respectively. Taking advantage of these findings, we targeted polymers containing two segments with distinct composition profiles from the same monomer feed ($f_{AA,0}$ = 0.1) and in one pot by changing α_{AA} *in situ* during polymerization. As a proof of concept, two experiments (called "Rich-end" and "Rich-start") were performed in which α was changed *in situ* at conversion ~50 % from 0 to 0.6 or from 0.6 to 0 by addition of small amounts of NaOH or HCl respectively (**Table S4**).

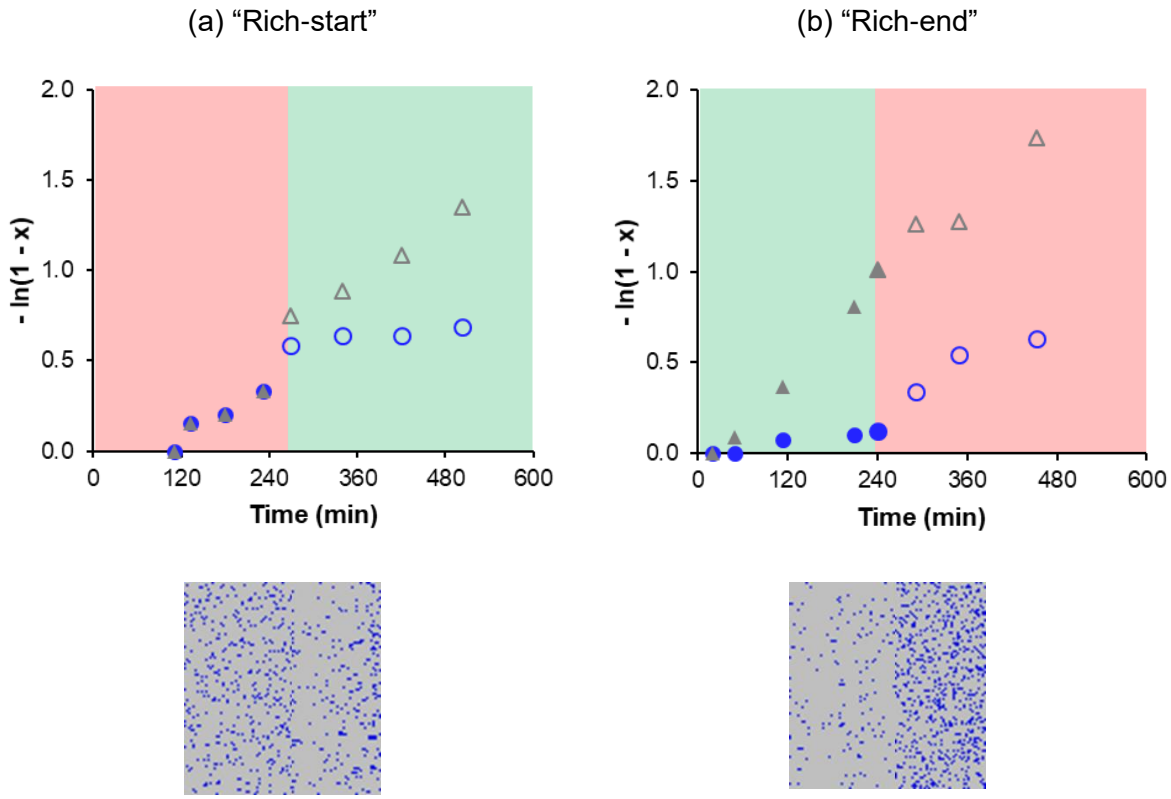

Figure 5. (top) Kinetic monitoring of the logarithmic conversions in MEA (Δ) and AA (○) for the two-step syntheses (a) Rich-start and (b) Rich-end (see **Table S4**). The full symbols refer to the first step (before changing α_{AA}) and the empty ones to the second step (after changing α_{AA}). The red and green areas correspond to α_{AA} = 0 and 0.60 respectively. (bottom) Simulated monodisperse copolymer chains (*DP* = 100) by changing the apparent

reactivity ratio of MEA when x_{global} reached 50%. Chains are stacked horizontally. The chain end is on the right side, the MEA units in grey and the AA in blue. Experimental $DP_{n\,0}$, $f_{AA,0}$, apparent reactivity ratios of MEA and the final global conversion were used for each step in the terminal model to determine the composition profiles (see SI).

Figure 5 shows that the relative rate of polymerization of each comonomer was strongly impacted when the NaOH or HCl solution was added in the reaction medium. The apparent reactivity ratio of MEA in each polymerization step could be estimated from the individual monomer conversions (**Figure S12** top). A clear influence of α_{AA} on r_{MEA} was found, as expected. For sample Rich-start, the polymerization rates of MEA and AA were similar at $\alpha_{AA} = 0$ until the addition of NaOH which caused the rate of polymerization of AA to decrease significantly while that of MEA stayed almost unchanged. After 24 h, the conversion in AA was < 25 % whereas MEA reached almost full conversion (see **Figure 5a**). On addition of NaOH, the turbid reaction medium became almost clear, but the polymer chains remained aggregated at the nano-scale as assessed by dynamic light scattering where tiny aggregates of around 20 nm in diameter were measured (D_h ~ 20 nm). For sample Rich-end, the synthesis started at $\alpha_{AA} = 0.60$. The polymerization reached ~ 50 % global conversion when the AA conversion was only 9 %. On addition of HCl, the dispersion became more turbid and both monomers polymerized with similar apparent first-order rate constants, as indicated by the parallel slopes of the first-order kinetic plots for each monomer (**Figure 5a**). Both monomers eventually reached quantitative conversion. SEC characterizations, displayed in **Figure S12** (bottom), showed that the overall control over the polymerization remained good.

Overall, these results demonstrate that the addition of tiny volumes of acid or base during polymerization can be used to modify the incorporation of AA and thereby the composition profile of the copolymers.

1.4. Influence of the distribution of AA units in the chain on their thermoresponsive properties

The insertion of hydrophilic monomers in thermoresponsive polymers is frequently used to modify their transition temperature[2,60–62], while the use of weakly acidic or basic monomers induces pH-sensitivity. Although PMEA is insoluble in water, triblock copolymers containing lateral PMEA blocks exhibited temperature-responsive rheological behaviour in water,[35] while block and gradient copolymers of MEA with hydrophilic hydroxyethyl acrylate (HEA) showed typical LCST behavior.[63]

We hypothesized that the thermosensitivity can be strongly influenced by the composition profile of the polymer chains[3], *i.e.* the position and the distribution of the hydrophilic moieties and/or of the charges, when the pH is high enough. Indeed, aqueous solutions of all P(MEA-*co*-AA) copolymers showed temperature-dependent changes in turbidity. For comparison, a PMEA homopolymer of similar DP_n (= 95) was insoluble over the whole temperature range. We therefore performed turbidimetry measurements between 5 °C and 70 °C on 3 wt% aqueous solutions of five copolymers with similar overall AA content (F_{AA} between 0.06 and 0.08) but different composition profiles: Rich-end (block-like), Rich-start (block-like), A-0bis (random), A-03 (moderate gradient) and A-1 (strong gradient) (see **Table S5**). The α_{AA} for the block-like copolymers could not be precisely determined due to their low AA content (which makes α_{AA} very sensitive to errors in the volume of acid or base added). Although different AA copolymers may show differences in α_{AA} at the same pH, depending on the local environment of the AA units[64], these differences should be relatively small for the copolymers analysed here, because the overall concentration of AA is low and thus, each individual AA unit is typically surrounded by MEA units. We therefore performed turbidimetry measurements at controlled pH (6, 4 and 2, see **Figure S13**). At pH 6, which corresponds to a high degree of AA deprotonation, all samples except A-1 formed nanometric micelles over the whole temperature range (Dz ≤ 20 nm obtained by DLS), leading to transparent solutions. Sample A-1, with a strong gradient structure and the lowest

overall AA content (F_{AA} = 0.057), scattered light strongly, indicating the presence of objects much larger than 20 nm, even at low temperature.

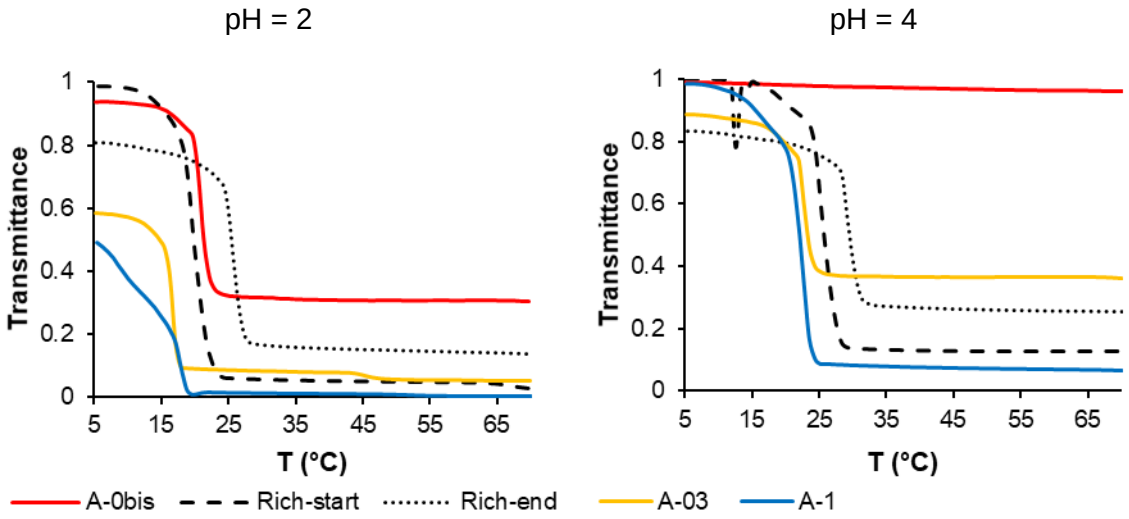

Figure 6. Evolution of the transmittance of 3 wt% copolymer aqueous solutions as a function of temperature (the first heating step is displayed). Full measurements are shown in **Figure S13**.

As summarized in **Figure 6**, distinct temperature behaviours were observed at pH = 2 (near-complete AA protonation) depending on the composition profile of the copolymers. All samples revealed an LCST-like transition between 15 and 25 °C: polymer chains aggregated into large particles lowering the transmittance when the temperature increased. Upon cooling, the reverse transition occurred systematically at slightly lower temperature (hysteresis of around 5 °C (**Figure S13**). The two gradient copolymers A-03 and A-1 were not completely soluble even at low temperature. For these copolymers, the transmittance further decreased with increasing temperature, quite sharply for A-03, and more progressively for the stronger gradient copolymer A-1. The block-like and the random copolymers (Rich-end, Rich-start and A-0bis, respectively) exhibited sharp LCST-type transitions between 20 and 25°C depending on the structure. A-0bis and Rich-start exhibited very similar behavior, which is consistent with their similar composition profiles (cf. Figures 3a and 5a). These two polymers were less turbid at low temperature than Rich-end, even though they contain less AA (F_{AA} = 0.062 for Rich-start

and 0.072 for A-0bis, vs. 0.078 for Rich-end). The temperature transition of Rich-start and A-0bis occurred at lower–temperature (around 20°C) compared to Rich-end (25°C). As expected[8], partial ionization of AA by increasing pH to 4 increased the solubility of the chains and thus, increased the cloud points by a few degrees (see **Table S5**) or even suppressed the transition for the random copolymer A-0bis. Overall, these results show that small changes in the composition profile of P(MEA-*co*-AA) copolymers have a strong effect on their thermoresponsiveness in water.

Conclusions.

The aim of this study was to control the incorporation of pH-sensitive AA in copolymers and to rely on this to control the composition profile of AA-containing copolymers through the simple modification of pH in aqueous RAFT dispersion polymerization. The idea was to change the apparent reactivity ratios of the comonomers by tuning the degree of ionization (α_{AA}) of AA. This study relies on the use of a heterogeneous polymerization process, where differences in intrinsic reactivity were amplified by differences in the partitioning of the comonomers between the continuous (aqueous solution) and discrete (polymer particle) phases, resulting in a strong change of apparent reactivity ratios. As a proof of concept, we studied the RAFT-mediated copolymerization of MEA and AA in aqueous dispersion over the whole range of α_{AA}. A novel trithiocarbonate RAFT agent functionalized by a sulfonate group was therefore synthesized to ensure water solubility over a broad pH range and good control over the polymerization. As expected, the apparent reactivity of AA dropped when α_{AA} was increased, switching from a random copolymerization to a gradient one. The observed change in apparent reactivity was much stronger than what would be expected from the change in intrinsic reactivity caused by ionization of AA. The additional contribution to the decrease in apparent reactivity of AA stemmed from the heterogeneous polymerization conditions leading to different partitioning of the comonomers: as the hydrophobic chains aggregate into particles, the comonomers must partition between the aqueous phase and the dispersed polymer phase. As a consequence, we propose that the monomer fraction of charged NaA in the polymer phase (which is the main locus of polymerization) is reduced relative to the continuous phase. This physical effect is more significant than the ionization-induced change in intrinsic

reactivity in the copolymerization of MEA and AA and becomes even more important when AA is copolymerized with a more hydrophobic monomer (MA). The strong effect of α_{AA} in heterogeneous aqueous copolymerizations was then exploited to synthesize block-like copolymers with different composition profiles from an identical monomer feed by changing the pH of the reaction medium *in situ*. This process was used to obtain copolymers that exhibited different thermoresponsive behaviors in aqueous dispersion despite their similar global composition. We thus showed that the composition profile, or equivalently the distribution of negative charges in a polymer chain, had a great impact on the macroscopic properties of the polymers, such as the thermo-sensitivity. Overall, improved understanding of the copolymerization of MEA with AA as a model pH-sensitive hydrophilic monomer, in complex dispersion polymerization conditions, should pave the way towards pH-sensitive copolymers with controlled composition profiles and stimuli-sensitivity.

Supporting Information.

The Supporting Information is available free of charge at XXX.

Experimental section including materials, synthesis protocols, characterization methods and complete characterizations of the RAFT agent and all polymers (including kinetic monitoring of the polymerizations). Description of the methods used to calculate the ionization degree, reactivity ratios (Jaacks method) and to simulate the copolymerization of MEA and AA using the terminal model. Discussion of the results of the copolymerization of AA with OEGA and MA (including SEC characterization and Jaacks plots) and the synthesis of "block-like" copolymers by changing α_{AA} *in situ.* Additional characterizations of the thermo-responsive properties of the samples by turbidimetry (including reversibility of the transition) and table summarizing the results. Calculation of the theoretically expected fraction of dead chains, and deconvolution of SEC chromatograms to estimate experimentally the fraction of dead chains.

Acknowledgments.

This work was funded by the Agence Nationale de la Recherche in the framework of the DYNAMIC-PISA ANR project (ANR-19-CE06-0002).

References.

(1) O'Lenick, T. G.; Jin, N.; Woodcock, J. W.; Zhao, B. Rheological Properties of Aqueous Micellar Gels of a Thermo- and PH-Sensitive ABA Triblock Copolymer. *J. Phys. Chem. B* **2011**, *115* (12), 2870–2881. https://doi.org/10.1021/jp2001332.

(2) Audureau, N.; Veith, C.; Coumes, F.; Nguyen, T. P. T.; Rieger, J.; Stoffelbach, F. RAFT-Polymerized N-Cyanomethylacrylamide-Based (Co)Polymers Exhibiting Tunable UCST Behavior in Water. *Macromol. Rapid Commun.* **2021**, *n/a* (n/a), 2100556. https://doi.org/10.1002/marc.202100556.

(3) Zhang, J.; Farias-Mancilla, B.; Kulai, I.; Hoeppener, S.; Lonetti, B.; Prévost, S.; Ulbrich, J.; Destarac, M.; Colombani, O.; Schubert, U. S.; Guerrero-Sanchez, C.; Harrisson, S. Effect of Hydrophilic Monomer Distribution on Self-Assembly of a PH-Responsive Copolymer: Spheres, Worms and Vesicles from a Single Copolymer Composition. *Angew. Chem. Int. Ed.* **2021**, *60* (9), 4925–4930. https://doi.org/10.1002/anie.202010501.

(4) Mayo, F. R.; Lewis, F. M. Copolymerization. I. A Basis for Comparing the Behavior of Monomers in Copolymerization; The Copolymerization of Styrene and Methyl Methacrylate. *J. Am. Chem. Soc.* **1944**, *66* (9), 1594–1601. https://doi.org/10.1021/ja01237a052.

(5) Beginn, U. Gradient Copolymers. *Colloid Polym. Sci.* **2008**, *286* (13), 1465–1474. https://doi.org/10.1007/s00396-008-1922-y.

(6) Fujisawa, T.; Penlidis, A. Copolymer Composition Control Policies: Characteristics and Applications. *J. Macromol. Sci. Part A* **2008**, *45* (2), 115–132. https://doi.org/10.1080/10601320701786877.

(7) Matyjaszewski, K.; Ziegler, M. J.; Arehart, S. V.; Greszta, D.; Pakula, T. Gradient Copolymers by Atom Transfer Radical Copolymerization. *J. Phys. Org. Chem.* **2000**, *13* (12), 775–786. https://doi.org/10.1002/1099-1395(200012)13:12<775::AID-POC314>3.0.CO;2-D.

(8) Audureau, N.; Coumes, F.; Guigner, J.-M.; Guibert, C.; Stoffelbach, F.; Rieger, J. Dual Thermo- and PH-Responsive N-Cyanomethylacrylamide-Based Nano-Objects Prepared by RAFT-Mediated Aqueous Polymerization-Induced Self-Assembly. *Macromolecules* **2022**, *55* (24), 10993–11005. https://doi.org/10.1021/acs.macromol.2c01953.

(9) Charbonneau, C.; De Souza Lima, M. M.; Chassenieux, C.; Colombani, O.; Nicolai, T. Structure of PH Sensitive Self-Assembled Amphiphilic Di- and Triblock Copolyelectrolytes: Micelles, Aggregates and Transient Networks. *Phys. Chem. Chem. Phys.* **2013**, *15* (11), 3955. https://doi.org/10.1039/c3cp43653e.

(10) Charbonneau, C.; Chassenieux, C.; Colombani, O.; Nicolai, T. Controlling the Dynamics of Self-Assembled Triblock Copolymer Networks via the PH. *Macromolecules* **2011**, *44* (11), 4487–4495. https://doi.org/10.1021/ma2002382.

(11) Shedge, A.; Colombani, O.; Nicolai, T.; Chassenieux, C. Charge Dependent Dynamics of Transient Networks and Hydrogels Formed by Self-Assembled PH-Sensitive Triblock Copolyelectrolytes. *Macromolecules* **2014**, *47* (7), 2439–2444. https://doi.org/10.1021/ma500318m.

(12) Coudert, N.; Debrie, C.; Harrisson, S.; Rieger, J.; Nicolai, T.; Colombani, O. Hydrogels of Amphiphilic Triblock Copolymers with Independently Tunable PH and Temperature-Controlled Exchange Dynamics. submitted to *Macromolecules* **2023** (manuscript ma-2023-01448f, under revision).

(13) Thompson, K.; Michielsen, S. Novel Synthesis of N-Substituted Polyacrylamides: Derivatization of Poly(Acrylic Acid) with Amines Using a Triazine-Based Condensing Reagent. *J. Polym. Sci. Part Polym. Chem.* **2006**, *44* (1), 126–136. https://doi.org/10.1002/pola.21042.
(14) Adili, A.; Korpusik, A. B.; Seidel, D.; Sumerlin, B. S. Photocatalytic Direct Decarboxylation of Carboxylic Acids to Derivatize or Degrade Polymers. *Angew. Chem. Int. Ed.* **2022**, *61* (40), e202209085. https://doi.org/10.1002/anie.202209085.
(15) Korpusik, A. B.; Adili, A.; Bhatt, K.; Anatot, J. E.; Seidel, D.; Sumerlin, B. S. Degradation of Polyacrylates by One-Pot Sequential Dehydrodecarboxylation and Ozonolysis. *J. Am. Chem. Soc.* **2023**, *145* (19), 10480–10485. https://doi.org/10.1021/jacs.3c02497.
(16) Yan, B.; Tao, L.-Z.; Liang, Y.; Xu, B.-Q. Sustainable Production of Acrylic Acid: Catalytic Performance of Hydroxyapatites for Gas-Phase Dehydration of Lactic Acid. *ACS Catal.* **2014**, *4* (6), 1931–1943. https://doi.org/10.1021/cs500388x.
(17) Stahl, G. A. Influence of Solvents on the Copolymerization of Acrylic Acid. *J. Polym. Sci. Polym. Lett. Ed.* **1980**, *18* (12), 811–814. https://doi.org/10.1002/pol.1980.130181211.
(18) Chernikova, E. V.; Zaitsev, S. D.; Plutalova, A. V.; Mineeva, K. O.; Zotova, O. S.; Vishnevetsky, D. V. Control over the Relative Reactivities of Monomers in RAFT Copolymerization of Styrene and Acrylic Acid. *RSC Adv.* **2018**, *8* (26), 14300–14310. https://doi.org/10.1039/C8RA00048D.
(19) Couvreur, L.; Lefay, C.; Belleney, J.; Charleux, B.; Guerret, O.; Magnet, S. First Nitroxide-Mediated Controlled Free-Radical Polymerization of Acrylic Acid. *Macromolecules* **2003**, *36* (22), 8260–8267. https://doi.org/10.1021/ma035043p.
(20) Lefay, C.; Charleux, B.; Save, M.; Chassenieux, C.; Guerret, O.; Magnet, S. Amphiphilic Gradient Poly(Styrene-Co-Acrylic Acid) Copolymer Prepared via Nitroxide-Mediated Solution Polymerization. Synthesis, Characterization in Aqueous Solution and Evaluation as Emulsion Polymerization Stabilizer. *Polymer* **2006**, *47* (6), 1935–1945. https://doi.org/10.1016/j.polymer.2006.01.034.
(21) Chapiro, A.; Dulieu, J.; Mankowski, Z.; Schmitt, N. Influence des solvants sur la copolymerisation de l'acide acrylique avec l'acrylonitrile et l'acrylamide. *Eur. Polym. J.* **1989**, *25* (9), 879–884. https://doi.org/10.1016/0014-3057(89)90104-3.
(22) Capasso Palmiero, U.; Chovancová, A.; Cuccato, D.; Storti, G.; Lacík, I.; Moscatelli, D. The RAFT Copolymerization of Acrylic Acid and Acrylamide. *Polymer* **2016**, *98*, 156–164. https://doi.org/10.1016/j.polymer.2016.06.024.
(23) Chapiro, A.; Le Doan Trung. Copolymerization of Acrylic and Methacrylic Acids with N-Vinylpyrrolidone. *Eur. Polym. J.* **1974**, *10* (11), 1103–1106. https://doi.org/10.1016/0014-3057(74)90076-7.
(24) Harrisson, S.; Ercole, F.; Muir, B. W. Living Spontaneous Gradient Copolymers of Acrylic Acid and Styrene: One-Pot Synthesis of PH-Responsive Amphiphiles. *Polym Chem* **2010**, *1* (3), 326–332. https://doi.org/10.1039/B9PY00301K.
(25) Universidad Autónoma Metropolitana-Iztapalapa, Depto. de Química, Área de Química Analítica, San Rafael Atlixco 186, Col. Vicentina, CP 09340 México, D. F., Mexico; Rojas-Hernández, A.; Ibarra-Montaño, E. L.; Rodríguez-Laguna, N.; Aníbal Sánchez-Hernández, A. Determination of PKa Values for Acrylic, Methacrylic and Itaconic Acids by 1H and 13C NMR in Deuterated Water. *J. Appl. Solut. Chem. Model.* **2015**, *4* (1), 7–18. https://doi.org/10.6000/1929-5030.2015.04.01.2.
(26) Cabaness, W. R.; Lin, T. Y.-C.; Párkányi, C. Effect of PH on the Reactivity Ratios in the Copolymerization of Acrylic Acid and Acrylamide. *J. Polym. Sci. [A1]* **1971**, *9* (8), 2155–2170. https://doi.org/10.1002/pol.1971.150090805.
(27) Ponratnam, S.; Kapur, S. L. Effect of PH on the Reactivity Ratios in Aqueous Solution Copolymerization of Acrylic Acid and N-Vinylpyrrolidone. *J. Polym. Sci. Polym. Chem. Ed.* **1976**, *14* (8), 1987–1992. https://doi.org/10.1002/pol.1976.170140815.
(28) Anseth, K. S.; Scott, R. A.; Peppas, N. A. Effects of Ionization on the Reaction Behavior and Kinetics of Acrylic Acid Polymerizations. *Macromolecules* **1996**, *29* (26), 8308–8312. https://doi.org/10.1021/ma960840r.

(29) Kabanov, V. A.; Topchiev, D. A.; Karaputadze, T. M. Some Features of Radical Polymerization of Acrylic and Methacrylic Acid Salts in Aqueous Solutions. *J. Polym. Sci. Polym. Symp.* **1973**, *42* (1), 173–183. https://doi.org/10.1002/polc.5070420120.
(30) Chaduc, I.; Crepet, A.; Boyron, O.; Charleux, B.; D'Agosto, F.; Lansalot, M. Effect of the PH on the RAFT Polymerization of Acrylic Acid in Water. Application to the Synthesis of Poly(Acrylic Acid)-Stabilized Polystyrene Particles by RAFT Emulsion Polymerization. *Macromolecules* **2013**, *46* (15), 6013–6023. https://doi.org/10.1021/ma401070k.
(31) *Acrylic acid and esters - Chemical Economics Handbook*. S&P Global. https://www.spglobal.com/commodityinsights/en/ci/products/acrylic-acid-acrylate-esters-chemical-economics-handbook.html (accessed 2023-06-20).
(32) Puig, J. E.; Corona-Galvan, S.; Maldonado, A.; Schulz, P. C.; Rodriguez, B. E.; Kaler, E. W. Microemulsion Copolymerization of Styrene and Acrylic Acid. *J. Colloid Interface Sci.* **1990**, *137* (1), 308–310. https://doi.org/10.1016/0021-9797(90)90068-Y.
(33) dos Santos, A. M.; McKenna, T. F.; Guillot, J. Emulsion Copolymerization of Styrene Andn-Butyl Acrylate in Presence of Acrylic and Methacrylic Acids: Effect of PH on Kinetics and Carboxyl Group Distribution. *J. Appl. Polym. Sci.* **1997**, *65* (12), 2343–2355. https://doi.org/10.1002/(SICI)1097-4628(19970919)65:12<2343::AID-APP8>3.0.CO;2-9.
(34) Shoaf, G. L.; Poehlein, G. W. Kinetics of Emulsion Copolymerization with Acrylic Acids. *J. Appl. Polym. Sci.* **1991**, *42* (5), 1213–1237. https://doi.org/10.1002/app.1991.070420506.
(35) Silva, F. M.; Lima, E. L.; Pinto, J. C. Acrylic Acid/Vinyl Acetate Suspension Copolymerizations. I. Partition Coefficients for Acrylic Acid. *J. Appl. Polym. Sci.* **2004**, *93* (3), 1077–1088. https://doi.org/10.1002/app.20538.
(36) Corona-Galvan, S.; Martinez-Gomez, A.; Castañeda-Perez, J.; Puig, J. E.; Schulz, P. C.; Dominguez, J. M.; Ruano, A. Effect of Emulsifier Type on the Copolymerization of Styrene and Acrylic Acid. *Polym. Eng. Sci.* **1991**, *31* (6), 404–409. https://doi.org/10.1002/pen.760310604.
(37) Santos, A. M.; Guillot, J.; McKenna, T. F. Partitioning of Styrene, Butyl Acrylate and Methacrylic Acid in Emulsion Systems. *Chem. Eng. Sci.* **1998**, *53* (12), 2143–2151. https://doi.org/10.1016/S0009-2509(98)00031-1.
(38) Zhang, H.-T.; Yuan, X.-Y.; Huang, J.-X. Study of Kinetics and Nucleation Mechanism of Dispersion Copolymerization of Methyl Methacrylate and Acrylic Acid. *React. Funct. Polym.* **2004**, *59* (1), 23–31. https://doi.org/10.1016/j.reactfunctpolym.2003.11.001.
(39) Zhang, X.; Boisson, F.; Colombani, O.; Chassenieux, C.; Charleux, B. Synthesis of Amphiphilic Poly(Acrylic Acid)-b-Poly(n-Butyl Acrylate-Co-Acrylic Acid) Block Copolymers with Various Microstructures via RAFT Polymerization in Water/Ethanol Heterogeneous Media. *Macromolecules* **2014**, *47* (1), 51–60. https://doi.org/10.1021/ma402125r.
(40) Coudert, N.; Debrie, C.; Rieger, J.; Nicolai, T.; Colombani, O. Thermosensitive Hydrogels of BAB Triblock Copolymers Exhibiting Gradually Slower Exchange Dynamics and an Unexpected Critical Reorganization Temperature Upon Heating. *Macromolecules* **2022**, *55* (23), 10502–10512. https://doi.org/10.1021/acs.macromol.2c01573.
(41) Sato, K.; Kobayashi, S.; Kusakari, M.; Watahiki, S.; Oikawa, M.; Hoshiba, T.; Tanaka, M. The Relationship Between Water Structure and Blood Compatibility in Poly(2-Methoxyethyl Acrylate) (PMEA) Analogues: The Relationship Between Water Structure and Blood Compatibility…. *Macromol. Biosci.* **2015**, *15* (9), 1296–1303. https://doi.org/10.1002/mabi.201500078.
(42) Tanaka, M.; Mochizuki, A. Effect of Water Structure on Blood Compatibility? Thermal Analysis of Water in Poly(Meth)Acrylate. *J. Biomed. Mater. Res.* **2004**, *68A* (4), 684–695. https://doi.org/10.1002/jbm.a.20088.
(43) Kurokawa, N.; Endo, F.; Bito, K.; Maeda, T.; Hotta, A. Antithrombogenic Poly(2-Methoxyethyl Acrylate) Elastomer via Triblock Copolymerization with Poly(Methyl Methacrylate). *Polymer* **2021**, *228*, 123876. https://doi.org/10.1016/j.polymer.2021.123876.
(44) Debrie, C.; Coudert, N.; Guigner, J.-M.; Nicolai, T.; Stoffelbach, F.; Colombani, O.; Rieger, J. Unimer Exchange Is Not Necessary for Morphological Transitions in Polymerization-Induced

Self-Assembly. *Angew. Chem. Int. Ed. n/a* (n/a), e202215134. https://doi.org/10.1002/anie.202215134.
(45) Liu, G.; Qiu, Q.; Shen, W.; An, Z. Aqueous Dispersion Polymerization of 2-Methoxyethyl Acrylate for the Synthesis of Biocompatible Nanoparticles Using a Hydrophilic RAFT Polymer and a Redox Initiator. *Macromolecules* **2011**, *44* (13), 5237–5245. https://doi.org/10.1021/ma200984h.
(46) Sugihara, S.; Ma'Radzi, A. H.; Ida, S.; Irie, S.; Kikukawa, T.; Maeda, Y. In Situ Nano-Objects via RAFT Aqueous Dispersion Polymerization of 2-Methoxyethyl Acrylate Using Poly(Ethylene Oxide) Macromolecular Chain Transfer Agent as Steric Stabilizer. *Polymer* **2015**, *76*, 17–24. https://doi.org/10.1016/j.polymer.2015.08.051.
(47) Mellot, G.; Guigner, J.-M.; Bouteiller, L.; Stoffelbach, F.; Rieger, J. Templated PISA: Driving Polymerization-Induced Self-Assembly towards Fibre Morphology. *Angew. Chem.* **2019**, *131* (10), 3205–3209. https://doi.org/10.1002/ange.201809370.
(48) Scheutz, G. M.; Bowman, J. I.; Mondal, S.; Rho, J. Y.; Garrison, J. B.; Korpanty, J.; Gianneschi, N. C.; Sumerlin, B. S. Gradient Copolymer Synthesis through Self-Assembly. *ACS Macro Lett.* **2023**, 454–461. https://doi.org/10.1021/acsmacrolett.3c00148.
(49) Stoffelbach, F.; Tibiletti, L.; Rieger, J.; Charleux, B. Surfactant-Free, Controlled/Living Radical Emulsion Polymerization in Batch Conditions Using a Low Molar Mass, Surface-Active Reversible Addition-Fragmentation Chain-Transfer (RAFT) Agent. *Macromolecules* **2008**, *41* (21), 7850–7856. https://doi.org/10.1021/ma800965r.
(50) Neal, T. J.; Penfold, N. J. W.; Armes, S. P. Reverse Sequence Polymerization-Induced Self-Assembly in Aqueous Media. *Angew. Chem. Int. Ed.* **2022**, *61* (33), e202207376. https://doi.org/10.1002/anie.202207376.
(51) Baussard, J.-F.; Habib-Jiwan, J.-L.; Laschewsky, A.; Mertoglu, M.; Storsberg, J. New Chain Transfer Agents for Reversible Addition-Fragmentation Chain Transfer (RAFT) Polymerisation in Aqueous Solution. *Polymer* **2004**, *45* (11), 3615–3626. https://doi.org/10.1016/j.polymer.2004.03.081.
(52) Mertoglu, M.; Laschewsky, A.; Skrabania, K.; Wieland, C. New Water Soluble Agents for Reversible Addition−Fragmentation Chain Transfer Polymerization and Their Application in Aqueous Solutions. *Macromolecules* **2005**, *38* (9), 3601–3614. https://doi.org/10.1021/ma048268o.
(53) Thomas, D. B.; Convertine, A. J.; Myrick, L. J.; Scales, C. W.; Smith, A. E.; Lowe, A. B.; Vasilieva, Y. A.; Ayres, N.; McCormick, C. L. Kinetics and Molecular Weight Control of the Polymerization of Acrylamide via RAFT. *Macromolecules* **2004**, *37* (24), 8941–8950. https://doi.org/10.1021/ma048199d.
(54) Gondi, S. R.; Rissing, C. J.; Son, D. Y. A Convenient Synthesis of Thiol, Trithiocarbonate and Disulfide. *ChemRxiv* **2021**. This content is a pre-print and has not been peer-reviewed. https://doi.org/10.26434/chemrxiv-2021-rrmw2-v2.
(55) Ye, Y. K.; Stringham, R. W. Effect of Mobile Phase Acidic Additives on Enantioselectivity for Phenylalanine Analogs. *J. Chromatogr. A* **2001**, *927* (1), 47–52. https://doi.org/10.1016/S0021-9673(01)01060-3.
(56) Bowman, J. I.; Eades, C. B.; Korpanty, J.; Garrison, J. B.; Scheutz, G. M.; Goodrich, S. L.; Gianneschi, N. C.; Sumerlin, B. S. Controlling Morphological Transitions of Polymeric Nanoparticles via Doubly Responsive Block Copolymers. *Macromolecules* **2023,** *56* (9), 3316-3323. https://doi.org/10.1021/acs.macromol.3c00445.
(57) Rinaldi, D.; Hamaide, T.; Graillat, C.; D'Agosto, F.; Spitz, R.; Georges, S.; Mosquet, M.; Maitrasse, P. RAFT Copolymerization of Methacrylic Acid and Poly(Ethylene Glycol) Methyl Ether Methacrylate in the Presence of a Hydrophobic Chain Transfer Agent in Organic Solution and in Water. *J. Polym. Sci. Part Polym. Chem.* **2009**, *47* (12), 3045–3055. https://doi.org/10.1002/pola.23374.

(58) Jaacks, V. A Novel Method of Determination of Reactivity Ratios in Binary and Ternary Copolymerizations. *Makromol. Chem.* **1972**, *161* (1), 161–172. https://doi.org/10.1002/macp.1972.021610110.
(59) Lacík, I.; Beuermann, S.; Buback, M. PLP-SEC Study into the Free-Radical Propagation Rate Coefficients of Partially and Fully Ionized Acrylic Acid in Aqueous Solution. *Macromol. Chem. Phys.* **2004**, *205* (8), 1080–1087. https://doi.org/10.1002/macp.200300251.
(60) Audureau, N.; Coumes, F.; Guigner, J.-M.; Nguyen, T. P. T.; Ménager, C.; Stoffelbach, F.; Rieger, J. Thermoresponsive Properties of Poly(Acrylamide-Co-Acrylonitrile)-Based Diblock Copolymers Synthesized (by PISA) in Water. *Polym. Chem.* **2020**, *11* (37), 5998–6008. https://doi.org/10.1039/D0PY00895H.
(61) Audureau, N.; Coumes, F.; Rieger, J.; Stoffelbach, F. Poly(N-Cyanoethylacrylamide), a New Thermoresponsive Homopolymer Presenting Both LCST and UCST Behavior in Water. *Polym. Chem.* **2022,** *13* (8), 1075-1083. https://doi.org/10.1039/D2PY00032F.
(62) Barker, I. C.; Cowie, J. M. G.; Huckerby, T. N.; Shaw, D. A.; Soutar, I.; Swanson, L. Studies of the "Smart" Thermoresponsive Behavior of Copolymers of N-Isopropylacrylamide and N,N-Dimethylacrylamide in Dilute Aqueous Solution. *Macromolecules* **2003**, *36* (20), 7765–7770. https://doi.org/10.1021/ma034250m.
(63) Steinhauer, W.; Hoogenboom, R.; Keul, H.; Moeller, M. Block and Gradient Copolymers of 2-Hydroxyethyl Acrylate and 2-Methoxyethyl Acrylate via RAFT: Polymerization Kinetics, Thermoresponsive Properties, and Micellization. *Macromolecules* **2013**, *46* (4), 1447–1460. https://doi.org/10.1021/ma302606x.
(64) Farias-Mancilla, B.; Zhang, J.; Kulai, I.; Destarac, M.; Schubert, U. S.; Guerrero-Sanchez, C.; Harrisson, S.; Colombani, O. Gradient and Asymmetric Copolymers: The Role of the Copolymer Composition Profile in the Ionization of Weak Polyelectrolytes. *Polym. Chem.* **2020**, *11* (47), 7562–7570. https://doi.org/10.1039/D0PY01059F.